Abdominal Radiology (2019) 44:984–991
https://doi.org/10.1007/s00261-018-1837-0

PANCREAS

Quantification and differentiation of composition of mixed pancreatic duct stones using single-source dual-energy CT: an ex vivo study

Ri Liu[1] · Weiwei Su[2] · Xingbiao Chen[3] · Wei Yin[1] · Jing Gong[1] · Jianping Lu[1]

Published online: 24 November 2018

Abstract

Purpose To evaluate the feasibility of using single-source dual-energy CT (SS DECT) to quantify and differentiate calcium carbonate (CA) and non-calcium carbonate (NCA) components of pancreatic duct stones (PDS) with mixed composition.

Materials and methods A total of 12 PDS harvested from general surgery department in our hospital were analyzed with micro-CT as a reference standard for CA and NCA composition. These stones were placed in a TOS water phantom of 35 cm diameter to simulate standard adult body size. High- and low-energy image sets were acquired from SS DECT scans with high/low tube potential pairs of 80 kVp/140 kVp. All the image sets were imported into an in-house software for further post-processing. CT number ratio (CTR), defined as the ratio of the CT number at 80 kVp to 140 kVp was calculated for each pixel of the images. Threshold was preset between 1.00 and 1.25 to classify CA and NCA components. Pixels in PDS with CTR higher than the threshold were classified as CA, and those with CTR lower than the threshold were classified as NCA. The percentages of CA and NCA for each stone were determined by calculating the number of CA and NCA pixels. Finally, the minimal, maximal and root-mean-square errors (RMSE) of composition measured by SS DECT under each threshold were calculated by referring to the composition data from micro-CT. The optimal threshold was determined with the minimal RMSE. A paired *t* test was used to compare the stone composition determined by DECT with micro-CT.

Results The optimal CTR threshold was 1.16, with RMSE of 6.0%. The minimum and maximum absolute errors were 0.22% and 11.35%, respectively. Paired *t* test showed no significant difference between DECT and micro-CT for characterizing CA and NCA composition ($p = 0.414$).

Conclusion SS DECT is a potential approach for quantifying and differentiating CA and NCA components in PDS with mixed composition.

Keywords Pancreatic duct stones · Single-source dual-energy CT · Micro-CT · Calcium carbonate · Non-calcium carbonate

Introduction

Pancreatic duct stone (PDS) is the most common pathological characteristic of chronic pancreatitis (CP), with an incidence of 50–90% in CP patients in western countries

Ri Liu, Weiwei Su and Xingbiao Chen contributed equally to the work.

✉ Jing Gong
gong.jing1980@163.com

✉ Jianping Lu
cjr.lujianping@vip.163.com

Ri Liu
liuri007@126.com

Weiwei Su
susmmu@163.com

Xingbiao Chen
xingbiao.chen@hotmail.com

Wei Yin
yinwei_0816@163.com

Extended author information available on the last page of the article

[1]. Extracorporeal shock wave lithotripsy (ESWL) is preferred as the first-line treatment prior to endoscopic retrograde cholangiopancreatography (ERCP) for PDS > 5 mm [2], but shows multifarious treatment responses in different individuals. Few reports [3, 4] have endeavored to predict ESWL efficacy for PDS patients utilizing non-contrast computed tomography (NCCT) parameters, which are dominated by density-related indexes such as Hounsfield units (HU). Our former study [5] was the first report on the significance of mean stone density for ESWL treatment efficacy in PDS patients. Recent advanced studies [6, 7] on urinary calculi stated that the stone composition, which accounts for imaging density or gray scale based on X-ray attenuation, can determine stone hardness or fragility. Accurate preoperative information about the inner stone components can assist physicians in estimating susceptibility to fragmentation by lithotripsy, thus avoiding unnecessary invasive interventional procedures or treatment failure. However, there are very few studies on PDS composition, stratified as inorganics of calcium carbonate and organics of proteins and mucopolysaccharides, although it is speculated to play an equally significant role for optimal disease management.

Several imaging modalities have been used for characterizing stones. Conventional plain radiography is simple and widely available for detecting stone location and size, but cannot depict the inner structure of the stone with low resolution [8]. As an alternative method, high-resolution CT can differentiate uric acid (UA) stones from other types using CT attenuation value in HU [9, 10]. However, it was unreliable for routine clinical application owing to its limited accuracy in distinguishing sub-types of calcium-based stones with mixed composition due to the overlapping grayscale values [11]. Infrared spectroscopy (IR) was used as a reference in some studies [12, 13], but the spot sampling mode limited its application for stones with mixed compositions. In essence, the micro-CT scanner imaging principle is basically the same as the clinical CT scanner. The former has the advantage of high resolution. Instead, micro-CT can accurately determine proportions of minerals with different X-ray attenuation values, solely based on the grayscale segmentation principle on three-dimensional image stacks. Micro-CT has been used as a reference standard due to its capability of reflecting heterogeneity and the actual percentage of each component in mixed stones [14]. However, it is only suitable for isolated single stone. Dual-energy computed tomography (DECT), with two different energy levels for post-acquisition image processing, can differentiate materials with different atomic numbers but similar attenuation coefficients [15]. The pixel-to-pixel analyzing mode could avoid overlap among different materials on CT images. In an in vitro study by Ferrandino [16], DECT was able to identify the brushite, calcium, struvite, cysteine and UA contents in stones. Primak et al. [17] reported 92–100% accuracy in differentiating UA from non-UA stones with DECT.

The purpose of this ex vivo study was to investigate the capability and feasibility of DECT in differentiating and quantifying the CA and NCA components within PDS, with micro-CT as a reference standard. Accurate stone composition and CA structural details can provide more evidence for the treatment selection.

Materials and methods

Phantom design and micro-CT scans

A total of 12 human PDS (maximum diameter 10.59–13.53 mm; mean 12.40 mm) of mixed CA/NCA composition were harvested from general surgery department in our hospital. No internal review board approval was required for the phantom study. The CA and NCA proportions of all stones were previously verified by micro-CT as a reference standard. Scanning parameters for micro-CT using a Skyscan 1076 system (Bruker, Billerica, MA) were as follows: tube potential, 70 kV; 1.0 mm aluminum filter at the source (Fig. 1).

Prior to SS DECT scanning, each stone was placed into a water-filled TOS water phantom, with 35 cm lateral width, to eliminate surrounding air bubbles (Fig. 2).

SS DECT acquisition

DECT scans were performed by a trained CT technologist by using a 256-slice SS DECT scanner (Brilliance iCT, Philips Healthcare, Cleveland, Ohio). Dual-energy scan protocol was applied, and low/high tube voltage was set as 80 kVp/140 kVp to achieve the best X-ray spectra differentiation. Additional key parameters were gantry rotation time, 0.5 s; detector width, 16 × 0.625 mm; collimation, 10 mm; pitch, 0.19. The tube current was automatically set and with average value of 600 mAs for 80 kVp and 150 mAs for 140 kVp. Finally, all scanning images were reconstructed at 1 mm image thickness for both low- and high-energy datasets. All axial CT images were reconstructed using knowledge-based iterative reconstruction (IMR-level 1: Philips Healthcare).

Stone composition analysis

All reconstructed DICOM images were further analyzed with an in-house software coding using MATLAB (Matlab R2015b, Mathworks Inc). The stone was first segmented with CT value-based thresholding methods on low-energy images set. CT number ratio (CTR), which is defined as the

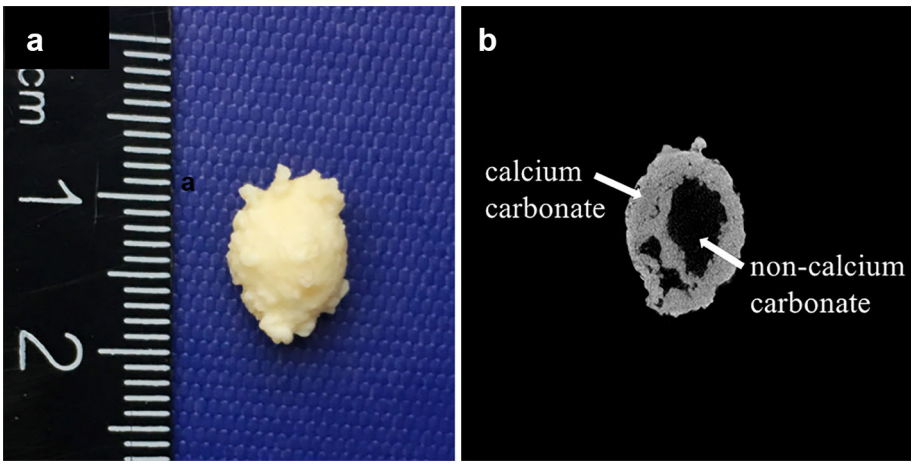

Fig. 1 Example of the ability to distinguish calcium carbonate (CA) and non-calcium carbonate (NCA) using micro-CT. **a** Photo of pancreatic stone, **b** micro-CT slice through the stone, showing CA (which has a characteristically high X-ray attenuation value) and NCA (which has a characteristically low X-ray attenuation value)

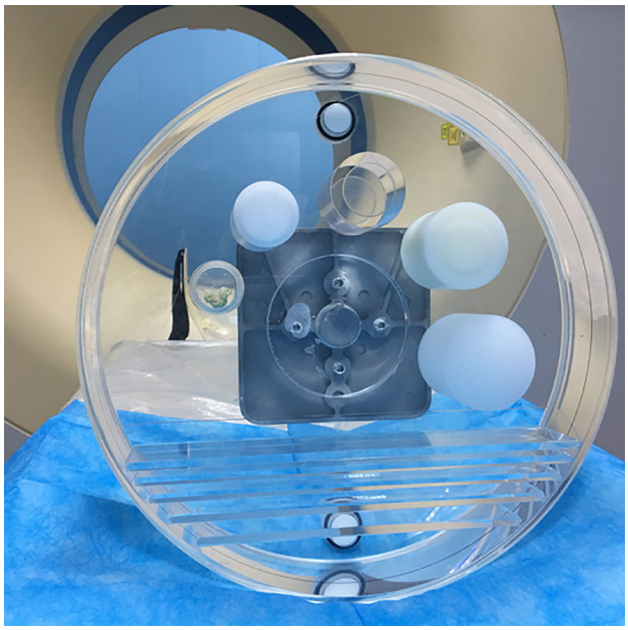

Fig. 2 Vitro pancreatic stone was placed into a TOS water phantom, with 35 cm lateral width

ratio of the CT number at the low to the high tube potential, was then calculated for each pixel of the stone. Based on preset thresholds, ranging from 1.00 to 1.25 with increment of 0.01, each pixel on CTR map was classified as CA (CTR > threshold) or NCA (CTR ≤ threshold). The percentage of CA and NCA for each stone was then calculated from the number of CA and NCA pixels in the whole stone. Consequently, each stone had a series of percentage numbers corresponding to the respective CTR thresholds (Figs. 3, 4).

Statistical analysis

SPSS statistics software (version 21.0, Chicago, III) was used for data analyses. As the mixed stones were divided into CA and NCA components, which had the same magnitude for the error as compared to the micro-CT reference standard, we chose the CA percentage in each stone for evaluating the difference between the two technologies. The root-mean-square error (RMSE) was calculated for each threshold to determine the optimal CTR threshold for recognizing CA composition. RMSE was calculated with the following formula:

$$\mathrm{RMSE} = \sqrt{\frac{1}{N}\sum_{i=1}^{N}\left(\mathrm{CA}_{\mathrm{DECT}} - \mathrm{CA}_{\mathrm{microCT}}\right)^2}$$

where N is the number of stones (12 in this study), $\mathrm{CA}_{\mathrm{DECT}}$ and $\mathrm{CA}_{\mathrm{microCT}}$ are the CA percentage obtained by SS DECT and micro-CT, respectively. The optimal CTR threshold was determined with minimal RMSE. With the optimal CTR threshold, the CA percentage calculated from SS DECT images was compared with that from micro-CT with paired t test, with $p < 0.05$ as statistically significant.

Results

Stone composition from micro-CT

PDS mean volume was 125.35 ± 115.41 mm^3, with range from 23.95 to 404.94 mm^3. The percentage of CA calculated by micro-CT ranged from 66.63% to 83.54%, and NCA from 33.37% to 16.46% (Table 1).

Stone composition by DECT

For each CTR threshold, CA and NCA percentages were calculated for every PDS, and RMSE was also calculated as compared to the CA percentage from micro-CT (Table 2). RMSE ranged from 6% to 16.96%, then decreased as CTR threshold increased from 1.00 to 1.16,

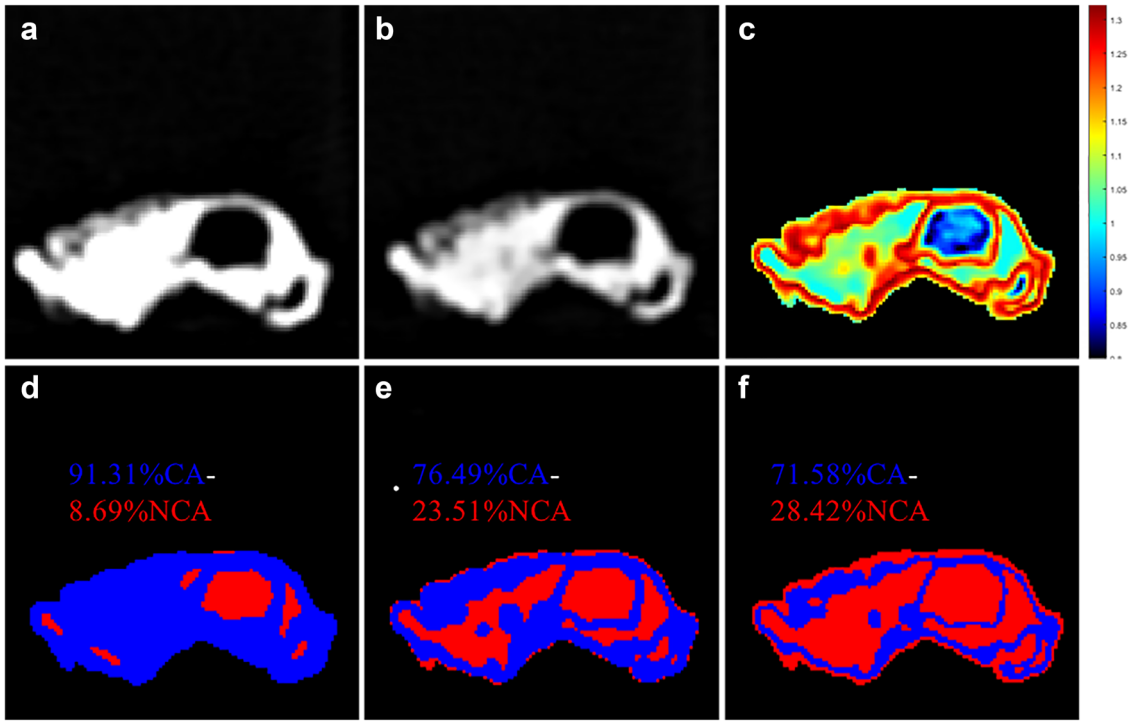

Fig. 3 Stone analysis example with SS DECT. Low- and high-energy CT images of a pancreatic stone (**a**, **b**), respectively, and the corresponding CTR color map (**c**). Composition maps show CA in blue and NCA in red, with CTR thresholds of 1.00 (**d**), 1.16 (**e**) and 1.20 (**f**). The error of CA estimation was 17.56% (**d**), 1.19% (**e**) and 7.84% (**f**) in comparison with the reference standard obtained from micro-CT (77.67% CA, 22.33% NCA)

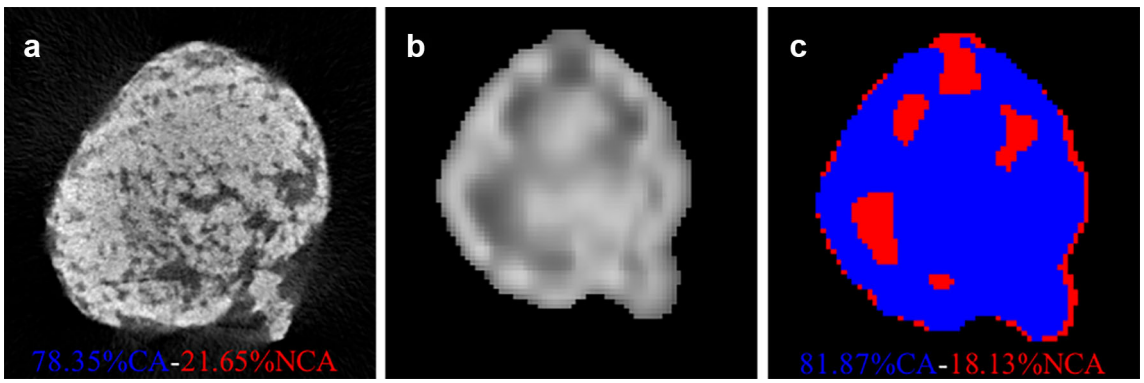

Fig. 4 Example of stone composition quantification with micro-CT image (**a**), mixed SS DECT images (**b**) and composition map from SS DECT (**c**)

and increased as CTR approached 1.25. The optimal CTR threshold was 1.16, corresponding to the minimal RMSE of 6% (Table 2, Fig. 5).

The images from one PDS are shown in Fig. 3, with the composition of 77.67% CA and 22.33% NCA predetermined by micro-CT as a reference standard.

With optimal CTR threshold of 1.16, CA percentage was calculated and compared with that from micro-CT using paired *t* tests, which showed no significant difference ($p = 0.414$). Images in Fig. 4 illustrate the comparison between micro-CT and SS DECT for a mixed PDS with optimal threshold of 1.16.

Discussion

ESWL is a widely accepted option for patients with urinary or pancreatic duct calculi, for which a preoperative assessment is essential because failure of ESWL may prolong patient suffering, waste medical resources and lead to financial burden. Previous studies on urinary calculi had

Table 1 Stone volume and composition determined by micro-CT

Stone no.	Volume (mm^3)	CA (%)	NCA (%)
1	209.68	66.63	33.37
2	206.23	74.72	25.28
3	50.09	74.50	25.50
4	56.46	74.73	25.27
5	39.81	75.57	24.43
6	48.65	83.54	16.46
7	104.82	77.67	22.33
8	54.00	78.35	21.65
9	23.95	78.39	21.61
10	69.73	73.29	26.71
11	404.94	73.98	26.02
12	235.79	73.40	25.60

uncovered many imaging factors correlated with ESWL outcome, such as stone size, location, number [18] and density-related indexes including mean or standard deviation of stone density (MSD or SDSD) [19], among which stone density (equal to HU) was the most important [20, 21]. It is widely acknowledged that stone density is internally determined by stone composition, which is the actual contributor for stone fragility and amenability to lithotripsy. There are a few reports on the significance of DECT in differentiating urinary stone types, but none on pancreatic stones. To the best of our knowledge, this is the first report utilizing DECT to identify PDS of mixed compositions. With the preset CTR threshold of 1.16, we obtained the minimal difference (6%) between DECT and micro-CT, which was smaller than the error in the study of Leng [22] for urinary stones. Our results indicate that DECT can accurately predict PDS stones in vitro and lay

Table 2 Stone composition by SS DECT under different CTR thresholds and corresponding RMSE with micro-CT

Ref.	Stone 1 74.72%	Stone 2 74.50%	Stone 3 74.73%	Stone 4 75.57%	Stone 5 83.54%	Stone 6 77.67%	Stone 7 78.35%	Stone 8 78.39%	Stone 9 73.29%	Stone 10 66.63%	Stone 11 73.98%	Stone 12 73.40%	RMSE
CTR													
1	88.76%	96.62%	84.93%	95.99%	96.43%	91.31%	90.65%	89.58%	95.95%	88.63%	87.37%	94.35%	16.96%
1.01	88.70%	96.43%	84.93%	95.30%	96.08%	90.65%	90.51%	89.30%	95.21%	88.17%	87.13%	93.81%	16.57%
1.02	88.26%	96.09%	83.84%	94.95%	95.37%	90.46%	90.08%	88.17%	94.47%	87.84%	86.63%	93.17%	16.06%
1.03	88.15%	95.66%	83.70%	93.90%	94.30%	89.90%	89.80%	87.61%	94.10%	87.32%	86.00%	92.32%	15.52%
1.04	87.65%	95.24%	82.74%	93.73%	93.23%	89.52%	89.52%	86.48%	93.37%	86.61%	85.36%	91.68%	14.95%
1.05	87.37%	94.66%	82.47%	93.21%	92.34%	88.48%	88.67%	85.35%	92.01%	85.79%	84.77%	90.83%	14.21%
1.06	86.98%	93.81%	81.51%	91.29%	91.44%	87.35%	88.53%	82.25%	91.65%	85.15%	84.23%	90.13%	13.40%
1.07	86.09%	93.19%	80.68%	89.55%	91.09%	86.31%	88.53%	81.41%	90.42%	84.41%	83.54%	89.71%	12.65%
1.08	85.25%	92.19%	80.00%	88.33%	89.13%	85.65%	88.53%	79.15%	89.56%	83.95%	83.00%	88.85%	11.90%
1.09	84.86%	91.09%	78.77%	87.11%	87.34%	85.17%	88.10%	77.46%	88.45%	83.07%	82.41%	87.79%	11.08%
1.1	84.42%	90.09%	78.22%	85.19%	86.45%	84.51%	87.25%	76.90%	86.86%	82.18%	81.62%	86.61%	10.16%
1.11	83.81%	89.09%	76.58%	83.62%	85.38%	83.29%	86.40%	75.77%	85.26%	81.51%	80.98%	85.65%	9.28%
1.12	83.31%	87.99%	75.21%	82.40%	83.07%	82.34%	85.41%	74.08%	83.66%	80.65%	80.44%	84.53%	8.48%
1.13	82.30%	86.76%	74.11%	81.18%	81.82%	80.83%	84.14%	71.83%	81.94%	79.86%	79.66%	83.89%	7.75%
1.14	81.86%	84.42%	72.88%	79.09%	80.21%	79.41%	83.43%	70.99%	80.10%	78.85%	78.53%	82.77%	6.86%
1.15	81.19%	82.09%	71.23%	78.05%	78.43%	77.53%	82.72%	69.30%	78.26%	77.96%	77.59%	81.23%	6.28%
1.16	80.47%	79.56%	68.90%	75.78%	77.90%	76.49%	81.87%	67.04%	76.41%	77.02%	76.66%	79.73%	6.00%
1.17	79.24%	77.80%	67.12%	72.82%	76.47%	75.45%	80.17%	64.51%	74.32%	76.34%	75.23%	78.77%	6.28%
1.18	78.30%	75.85%	64.79%	69.51%	75.40%	74.41%	77.76%	63.38%	71.87%	75.49%	73.76%	77.33%	6.76%
1.19	77.30%	73.51%	63.42%	66.20%	73.80%	73.56%	76.35%	61.13%	69.41%	74.60%	72.53%	75.95%	7.77%
1.2	76.52%	71.32%	61.23%	64.11%	72.73%	71.58%	74.65%	58.87%	66.71%	73.47%	71.25%	74.61%	9.01%
1.21	75.18%	68.94%	59.59%	62.72%	71.66%	69.78%	73.23%	57.75%	64.37%	72.25%	70.22%	73.28%	10.03%
1.22	73.62%	66.27%	57.12%	59.76%	69.70%	68.46%	71.39%	56.34%	62.65%	71.03%	69.14%	71.57%	11.54%
1.23	72.79%	63.46%	55.34%	58.89%	67.38%	67.33%	69.55%	52.68%	61.18%	69.74%	67.52%	69.92%	13.22%
1.24	71.90%	60.79%	54.52%	57.32%	65.42%	66.38%	69.12%	49.86%	58.85%	68.89%	66.19%	68.48%	14.69%
1.25	70.56%	58.31%	53.15%	55.40%	63.10%	64.78%	67.42%	47.32%	56.76%	67.60%	65.16%	66.19%	16.39%

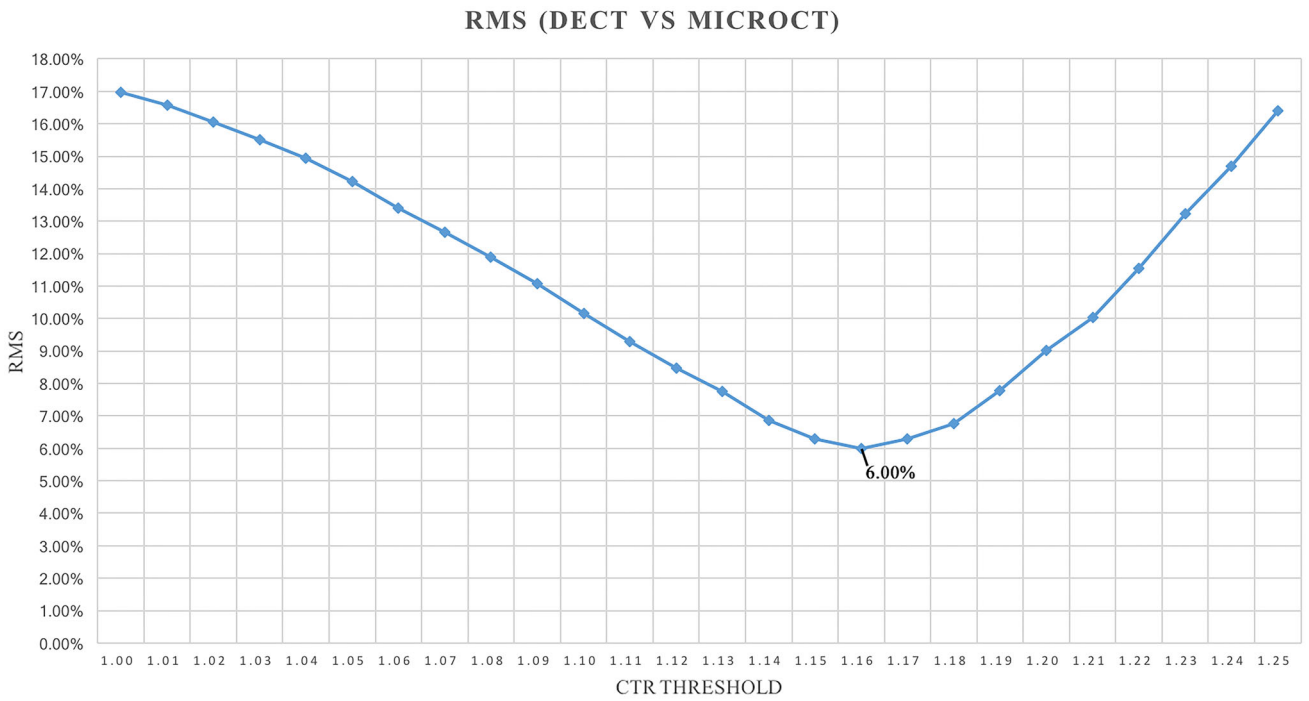

Fig. 5 Root-mean-square error (RMSE) variations along CTR threshold

the foundation for the clinical application of DECT to predict ESWL prognosis.

The stone compositions in the urinary system, which had relatively higher incidence and more complicated components than other systems, included calcium-oxalate stones (70%), calcium phosphate (20%), uric acid (UA) (10%), cystine, brushite and struvite [17]. A previous study had divided urinary stones into CA and NCA, or UA and NUA [23], but failed to clearly separate each component due to the diversity in mixed stones. In contrast, components in PDS are relatively simple, dominated by calcium carbonate (90%) and small proportion of proteins or mucopolysaccharides [24], which have distinctly different hardness and friability. The categorization could be easily established as CA and NCA, of which CA stones are hard and could be a major cause of failure of ESWL treatment. Based on similar mechanism, we speculated that PDS with high percentage of CA component is more resistant to ESWL fragmentation and may require other complementary or alternative therapies. In contrast, patients with PDS of NCA as the dominant component should be suitable candidates for ESWL. Clinical trials are required in the future to confirm this hypothesis.

There are four main technologies for DECT, both of which can identify the material based on two datasets with high and low energy levels. (1) Dual-source DECT has high temporal resolution by simultaneously acquisiting data using two X-ray tubes and detectors with different tube voltage and current. However, the limited central field of view decreases data accuracy; (2) rapid kV switching technique uses fast tube potential switching to allow alternate projection measurements under low and high tube potentials, and has a full 50-cm field of view available for data analysis. However, the overlap of energy spectra was relatively high; (3) dual-layer detector DECT employs two-layer detectors to simultaneously collect low- and high-energy data and can realize material decomposition in projection space, but also has relatively higher energy spectral overlap; (4) single-source sequential scanning DECT can perform two temporally sequential scans to obtain low- and high-energy data, but any patient motion occurring between the two scans may cause severe degradation of the resultant images and material composition [25–27]. Our Phantom test applied single-source sequential scanning DECT technique, since the phantom had no movement during two scans but can maintain the same high spatial resolution as conventional CT.

This study had several limitations. First, this was a phantom study, with a fixed water phantom simulating the normal adult body, but ignored the difference of X-ray penetration and spectral separation between different body shapes, which directly affect the composition calculation and the final optimal threshold [28]. Another study [22] designed a wide range of phantom sizes representing thin to very obese bodies and set five DS DECT scan modes based on the phantom size. Therefore, for extensive applicability of our hypothesis, further studies are required based on individualized phantoms. Second, the number of

stones included in this study was relatively small, which may lead to characteristic error for grouped comparison. The small sample size was due to the low incidence of PDS and the limited technological availability of micro-CT. The data were sufficient to account for our hypothesis. Although we had set a series of thresholds to determine the CTR with minimal RMSE with optimal accuracy, this in vitro study could not completely substitute the human body. Therefore, the present findings require confirmation from clinical trials in vivo. The investigation of PDS composition by DECT and the response to ESWL requires further study.

Conclusion

This ex vivo study for the first time demonstrated that SS DECT has the potential to be employed for CA and NCA composition differentiation, and to quantify the composition of combination calculus in a relatively accurate way with optimal CTR threshold of 1.16. Future in vivo studies would promote the clinical application of DECT in characterizing stone composition.

Author contributions WY is a trained CT technologist and made a significant contribution to this paper, including experiment, data processing.

Funding This study is not supported by any funding.

Compliance with ethical standards

Conflict of interest The authors have no potential conflict of interest to declare.

References

1. Sebastiano PD, Mola FFD, Büchler MW, et al. (2004) Pathogenesis of pain in chronic pancreatitis. Digestive Diseases 22(3):267–272
2. Dumonceau JM, Delhaye M, Tringali A, et al. (2012) Endoscopic treatment of chronic pancreatitis: European Society of Gastrointestinal Endoscopy (ESGE) Clinical Guideline. Endoscopy 44(08):784–800
3. Ohyama H, Mikata R, Ishihara T, et al. (2015) Efficacy of stone density on noncontrast computed tomography in predicting the outcome of extracorporeal shock wave lithotripsy for patients with pancreatic stones. Pancreas 44(3):422–428
4. Lapp RT, Wolf JS Jr, Faerber GJ, et al. (2016) Duct diameter and size of stones predict successful extracorporeal shock wave lithotripsy and endoscopic clearance in patients with chronic pancreatitis and pancreaticolithiasis. Pancreas 45(8):1208–1211
5. Liu R, Su W, Gong J, et al. (2018) Noncontrast computed tomography factors predictive of extracorporeal shock wave lithotripsy outcomes in patients with pancreatic duct stones. Abdominal Radiology 8207:1–7
6. Kijvikai K, Rosette JJMDL (2011) Assessment of stone composition in the management of urinary stones. Nature Reviews Urology 8(2):81–85
7. Williams JC, Zarse CA, Hameed TA, et al. (2007) CT visible internal stone structure, but not Hounsfield unit value, of calcium oxalate monohydrate (COM) calculi predicts lithotripsy fragility in vitro. Urological Research 35(4):201–206
8. Krishnamurthy MS, Ferucci PG, Sankey N, et al. (2005) Is stone radiodensity a useful parameter for predicting outcome of extracorporeal shockwave lithotripsy for stones $\leq$ 2 cm. International Brazilian Journal of Urology 31(1):3–8
9. Perks AE, Schuler TD, Lee J, et al. (2008) Stone attenuation and skin-to-stone distance on computed tomography predicts for stone fragmentation by shock wave lithotripsy. Urology 72(4):765–769
10. Sheir KZ, Mansour O, Madbouly K, et al. (2005) Determination of the chemical composition of urinary calculi by noncontrast spiral computerized tomography. Urological Research 33(2):99–104
11. Sotoodeh SP, Mehdi K, Bahman A, et al. (2014) The comparative survey of Hounsfield units of stone composition in urolithiasis patients. Journal of Research in Medical Sciences the Official Journal of Isfahan University of Medical Sciences 19(7):650–653
12. Li X, Zhao R, Liu B, et al. (2013) Gemstone spectral imaging dual-energy computed tomography: a novel technique to determine urinary stone composition. Urology 81(4):727–730
13. Qu M, Ramirez-Giraldo JC, et al. (2013) Urinary stone differentiation in patients with large body size using; dual-energy dual-source computed tomography. European Radiology 23(5):1408–1414
14. Zarse CA, Mcateer JA, Sommer AJ, et al. (2004) Nondestructive analysis of urinary calculi using micro computed tomography. BMC Urology 4(1):15
15. Pramanik R, Asplin JR, Jackson ME, et al. (2008) Protein content of human apatite and brushite kidney stones: significant correlation with morphologic measures. Urological Research 36(5):251
16. Ferrandino MN, Pierre SA, Simmons WN, et al. (2010) Dual-energy computed tomography with advanced postimage acquisition data processing: improved determination of urinary stone composition. Journal of Endourology 181(4):827
17. Primak AN, Fletcher JG, Vrtiska TJ, et al. (2007) Noninvasive differentiation of uric acid versus non-uric acid kidney stones using dual-energy CT. Academic Radiology 14(12):1441–1447
18. Kanao K, Nakashima J, Nakagawa K, et al. (2006) Preoperative nomograms for predicting stone-free rate after extracorporeal shock wave lithotripsy. Journal of Urology 176(4):1453–1457
19. Lee JY, Kim JH, Kang DH, et al. (2016) Stone heterogeneity index as the standard deviation of Hounsfield units: a novel predictor for shock-wave lithotripsy outcomes in *Ureter calculi*. Scientific Reports 6:23988
20. Graser A, Johnson TRC, Bader M, et al. (2008) Dual energy Ct characterization of *Urinary calculi*: initial in vitro and clinical experience. Investigative Radiology 43(2):112–119
21. Kambadakone AR, Eisner BH, Catalano OA, et al. (2010) New and evolving concepts in the imaging and management of

urolithiasis: urologists' perspective. Radiographics a Review Publication of the Radiological Society of North America Inc 30(3):603
22. Leng S, Huang A, Montoya J, et al. (2016) Quantification of urinary stone composition in mixed stones using dual-energy CT: a phantom study. AJR American Journal of Roentgenology 207(2):321
23. Mansouri M, Aran S, Singh A, et al. (2015) Dual-Energy computed tomography characterization of urinary calculi: basic principles, applications and concerns. Current Problems in Diagnostic Radiology 44(6):496–500
24. Farnbacher MJ, Voll RE, Faissner R, et al. (2005) Composition of clogging material in pancreatic endoprostheses. Gastrointestinal Endoscopy 61(7):862–866
25. Kulkarni NM, Eisner BH, Pinho DF, et al. (2013) Determination of renal stone composition in phantom and patients using single-source dual-energy computed tomography. Journal of Computer Assisted Tomography 37(1):37–45
26. Mccollough CH, Leng S, Yu L, et al. (2015) Dual- and, multi-energy CT: principles, technical approaches, and clinical applications. Radiology 276(3):637–653
27. Rassouli N, Etesami M, Dhanantwari A, et al. (2017) Detector-based spectral CT with a novel dual-layer technology: principles and applications. Insights into Imaging 8(6):589–598
28. Qu M, Ramirez-Giraldo JC, Leng S, et al. (2011) Dual-energy dual-source CT with additional spectral filtration can improve the differentiation of non-uric acid renal stones: an ex vivo phantom study. AJR American Journal of Roentgenology 196:1279–1287

Affiliations

Ri Liu[1] · Weiwei Su[2] · Xingbiao Chen[3] · Wei Yin[1] · Jing Gong[1] · Jianping Lu[1]

[1] Department of Radiology, Changhai Hospital Affiliated to the Naval Military Medical University, Changhai Road 168, Yangpu District, Shanghai 200433, People's Republic of China

[2] Department of Nuclear Medicine, Changhai Hospital Affiliated to the Naval Military Medical University, Changhai Road 168, Yangpu District, Shanghai 200433, People's Republic of China

[3] Clinical Science, Philips Healthcare, No 718 Lingshi Road, JingAn District, Shanghai 201100, People's Republic of China